



Diastereoselective synthesis of a “chiral-at-Ru” secondary phosphine complex

Gregory L. Gibson^a, Krista M.E. Morrow^a, Robert McDonald^b, Lisa Rosenberg^{a,*}

^aDepartment of Chemistry, University of Victoria, P.O. Box 3065, Victoria, BC, Canada V8W 3V6

^bX-ray Crystallography Laboratory, Department of Chemistry, University of Alberta, Edmonton, AB, Canada T6G 2G2

ARTICLE INFO

Article history:

Available online 30 December 2010

Dedicated to Professor Robert Bergman

Keywords:

Secondary phosphine complex
Ruthenium
Chiral-at-metal
Epimerization
Diastereoselectivity
NOESY NMR

ABSTRACT

Synthesis of the half-sandwich ruthenium complex $[\text{RuCl}(\eta^5\text{-indenyl})\{\text{P}(\text{Bu}^t)(\text{Ph})\text{H}\}(\text{PPh}_3)]$, **2**, containing an unsymmetrically-substituted secondary phosphine, is described. A 60:40 kinetic distribution of the resulting diastereomers **2a** and **2b** shifts in solution at room temperature to give predominantly **2a**. The relative stereochemistries at ruthenium and the secondary phosphine in each diastereomer have been assigned based on ¹H NOESY NMR and crystallographic data.

© 2010 Elsevier B.V. All rights reserved.

1. Introduction

We have previously described the synthesis of half-sandwich ruthenium complexes of symmetrically substituted secondary phosphines of the formula $[\text{Ru}(\eta^5\text{-indenyl})\text{Cl}(\text{PR}_2\text{H})(\text{PPh}_3)]$ [1]. Their subsequent dehydrohalogenation reactions generate highly reactive terminal phosphido complexes containing a Ru–PR₂ π-bond [2]. As shown in Scheme 1, these phosphido complexes react with alkyl halides, alkenes and alkynes to generate new P–C bonds, and we are currently pursuing the appropriate conditions to make these reactions catalytic, using $[\text{Ru}(\eta^5\text{-indenyl})\text{Cl}(\text{PPh}_3)_2]$, **1**, as a precatalyst.

This is a preliminary report of our efforts to extend this chemistry to the stereoselective P–C bond-forming reactions of unsymmetrically-substituted secondary phosphines. The chirality at ruthenium in the symmetric secondary phosphine complexes in Scheme 1 is evident from their ¹³C and ¹H NMR spectra, which show distinct chemical shifts for peaks due to the diastereotopic substituents at the coordinated secondary phosphine [1]. An intriguing strategy for the production/resolution of chiral phosphines would capitalize on this chirality through the selective enhancement of the rate of P–C bond formation for one of two diastereomers resulting from the addition of a racemic mixture of a P-chiral secondary phosphine to $[\text{Ru}(\eta^5\text{-indenyl})\text{Cl}(\text{PPh}_3)_2]$. Encouragingly, in this context, we report here the stereoselective synthesis of the mixed phosphine complex $[\text{Ru}(\eta^5\text{-indenyl})\text{Cl}\{\text{P}(\text{Bu}^t)-$

$(\text{Ph})\text{H}\}(\text{PPh}_3)]$, **2** (Scheme 2), and equilibration between the two diastereomers in solution, which leads to a thermodynamic product mixture of enhanced diastereomeric excess.

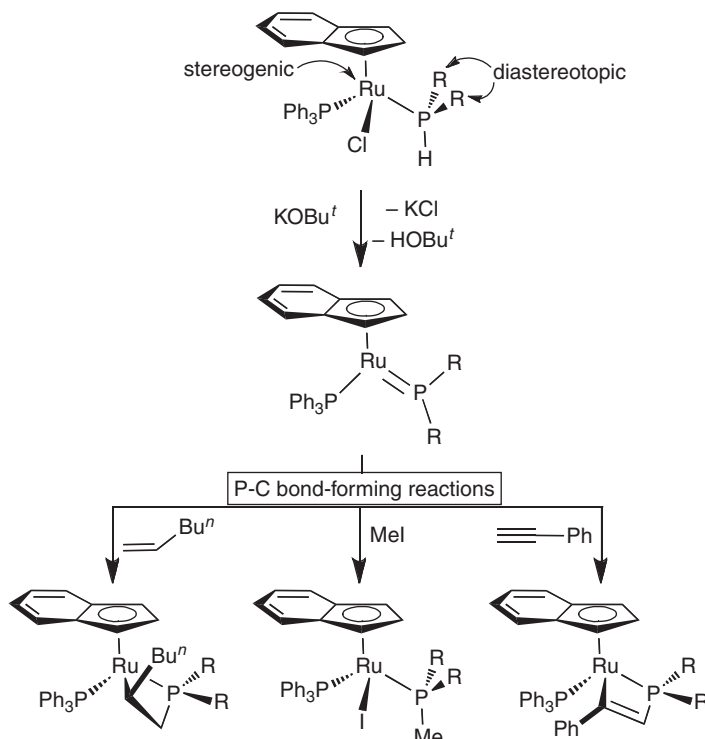
2. Experimental

2.1. General details

Unless otherwise noted, all reactions and manipulations were performed under nitrogen in an MBraun Unilab 1200/780 glovebox or using conventional Schlenk techniques. All solvents were sparged with nitrogen for 25 min and dried using an MBraun Solvent Purification System (SPS). Deuterated solvents were purchased from Cambridge Isotope Labs (CIL), freeze–pump–thaw degassed, and vacuum transferred from sodium/benzophenone (*d*₆-benzene, *d*₈-toluene) or calcium hydride (*d*-chloroform) before use. $[\text{RuCl}(\eta^5\text{-indenyl})(\text{PPh}_3)_2]$ was prepared as described previously [1]. H₂PBu^tPh was purchased from Sigma–Aldrich Canada and used as received. NMR spectra were recorded on a Bruker AVANCE 500 operating at 500.13 MHz for ¹H, 125.77 MHz for ¹³C, and 202.46 MHz for ³¹P, or on a Bruker AVANCE 300 operating at 300.13 MHz for ¹H, and 121.49 MHz for ³¹P. Chemical shifts are reported in ppm at ambient temperature unless otherwise noted. ¹H chemical shifts are referenced against residual protonated solvent peaks at 7.16 ppm (C₆D₅H) and 7.24 ppm (CHCl₃). ¹³C chemical shifts are referenced against CDCl₃ at 77.5 ppm. All ¹H, ¹³C chemical shifts are reported relative to tetramethylsilane (TMS), and ³¹P chemical shifts are reported relative to 85% H₃PO₄(aq.). Elemental analysis was performed by Canadian Microanalytical Service Ltd.,

* Corresponding author.

E-mail address: lisarose@uvic.ca (L. Rosenberg).



Scheme 1.

Delta, BC, Canada. IR spectra were recorded on a Perkin–Elmer FTIR Spectrum One spectrophotometer using KBr pellets under a nitrogen atmosphere.

2.2. Synthesis of $[\text{RuCl}(\eta^5\text{-indenyl})\{\text{P}(\text{Bu}^t)(\text{Ph})\text{H}\}(\text{PPh}_3)]$ (**2a** and **2b**)

$[\text{RuCl}(\eta^5\text{-indenyl})(\text{PPh}_3)_2]$ (**1**) (0.345 g, 0.44 mmol) and HPBu^tPh (0.155 g, 0.93 mmol) were added to a Schlenk flask with a stir bar. Dichloromethane (~30 mL) was added and the resulting dark red solution was refluxed for 3.75 h, at which point the solvent was removed under vacuum to give a dark red oil. Washing with hexanes (4×20 mL) gave an orange powder, which was isolated by filtration, and dried under vacuum. Crude yield: 0.151 g, 0.22 mmol, 50%. This powder was clean except for traces of residual PPh_3 , HPBu^tPh , and CH_2Cl_2 , and contained diastereomers **a** and **b** in a 60:40 ratio. A portion of the product was recrystallized by slow diffusion of hexanes into a concentrated dichloromethane solution. The resulting red crystals were used for both X-ray diffraction (Section 2.4) and elemental analysis.

IR (KBr, cm^{-1}): 2371 (w, $\nu_{\text{P-H}}$), 2338 (m, $\nu_{\text{P-H}}$); *Anal. Calc.* for $\text{C}_{37}\text{H}_{37}\text{ClP}_2\text{Ru} \cdot 0.33\text{CH}_2\text{Cl}_2$: C, 63.31; H, 5.36. Found: C, 63.75; H, 5.52%. Mp. 186 °C (decomposed).

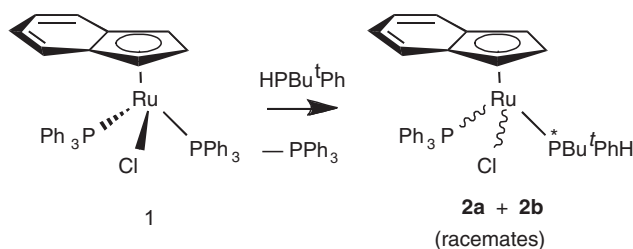
2.3. ^1H and $^{13}\text{C}\{^1\text{H}\}$ NMR data for **2a** and **2b**

Tables 1 and 2.

2.4. Reaction of $[\text{RuCl}(\eta^5\text{-indenyl})\{\text{P}(\text{Bu}^t)(\text{Ph})\text{H}\}(\text{PPh}_3)]$ (**2a** and **2b**) with KOBU^t

A powder sample of $[\text{RuCl}(\eta^5\text{-indenyl})\{\text{P}(\text{Bu}^t)(\text{Ph})\text{H}\}(\text{PPh}_3)]$ (**2a** and **2b**) (0.036 g, 0.053 mmol) and KOBU^t (0.008 g, 0.07 mmol)

¹ We have previously observed the tendency of these mixed phosphine complexes to retain solvent, even after prolonged drying under vacuum (see Ref. [1]); the ^1H NMR spectrum of the sample submitted for analysis does indicate the presence of residual dichloromethane.



Scheme 2.

were added to a Schlenk flask with a stir bar. The addition of toluene (~5 mL) gave an orange solution that began to darken to purple after about 5 min of stirring at room temperature. After 25 min of stirring the mixture was a deep blue color, with a yellow meniscus. At this point the solvent was removed under vacuum, leaving a dark green–yellow oil, which was dissolved in d_6 -benzene and analyzed by $^{31}\text{P}\{^1\text{H}\}$ NMR within 20 min. The spectrum showed some unreacted **2a** and **2b** (38%, 21:1 **a:b**), as well as signals assigned to two isomers of the corresponding terminal phosphido complexes **3** and **3'** (1:7.3), other signals assigned to the two phosphido decomposition products **4**, **4'** (16%, 1:1.3), and several unassigned signals (9%).

2.5. Crystallographic data

2.5.1. X-ray structure determination

Crystals of **2** were grown via slow diffusion of hexanes into a dichloromethane solution of the compound. Crystallographic experimental data and refinement details can be found in Table 3. All non-hydrogen atoms of the ruthenium complex molecule were refined with isotropic displacement parameters. Hydrogen atoms attached to carbons were assigned positions based on the idealized sp^2 or sp^3 geometries of their attached atoms, and were given thermal parameters 20% greater than those of the parent carbons. The hydrogen atom attached to phosphorus was located from a

Table 1
500 MHz ^1H NMR data at 300 K: δ in ppm (multiplicity, RI, J_{avg} or $\omega_{1/2}$ in Hz).

	η^5 -Indenyl					PPh ₃	HPBu ^t -Ph		Bu ^t
	H ₇ , H ₄	H ₆ , H ₅	H ₂	H ₃ , H ₁	Ph		P-H		
2a^a	7.76 (d, 1H, 8) 6.76 (d, 1H, 8) 6.90 (t, 1H, 8)	7.41 (t, 1H, 8) 6.90 (t, 1H, 8)	5.79–5.77 (m, 1H)	5.53–5.50 (m, 1H) 2.81 (s, 1H)	6.6 (br s, 110)	7.02–6.88 (om)	5.45 (dd, 363, 5)	1.27 (d, 9H, 14)	
2b^a	7.47 (d, 1H, 8) 6.93 (d, 1H, 7) 7.62 (d, 1H, 8) 6.50 (d, 1H, 8)	7.20 (t, 1H, 8) 7.11 (t, 1H, 8) 7.51 (t, 1H, 8) 6.94 (t, 1H, 8)	5.22–5.19 (m, 1H)	4.60 (s, 1H) 4.18 (s, 1H) 5.50 (br s, 1H, 9) 2.70 (br s, 1H, 5)	7.47 (br s, 22) 7.04–6.98 (om) For both isomers: 7.28–7.03 (om, some br) 6.32 (br s, 65) br in baseline	7.25–7.20 (m) 7.09–7.04 (m) 7.38–7.33 (m, overlaps H _{6/5} from b) 7.16–7.09 (m, overlaps PPh ₃) 7.27–7.22 (m, overlaps Ar massif) 7.16–7.11 (m, overlaps Ar massif)	5.51 (dd, 346, 6)	0.94 (d, 9H, 14)	
2b^b	7.50 (d, 1H, 8) 6.66 (d, 1H, 8)	7.34 (t, 1H, 8, overlaps PPh ₃) 7.00 (t, 1H, 8)	5.33 (br s, 1H, 7)	4.62 (br s, 1H, 7) 4.08 (br s, 1H, 6)	5.29 (dd, 1H, 346, 8)			0.92 (d, 9H, 14)	

^a Sample in *d*₆-benzene, aromatic assignments obtained indirectly from ^1H NOESY and COSY experiments.^b Sample in *d*₁-chloroform, aromatic assignments obtained indirectly from ^1H COSY, $^1\text{H}/^{13}\text{C}$ HSQC and HMBC experiments (see Table 2).

difference Fourier map, and its atomic coordinates and isotropic displacement parameter were allowed to freely refine. Attempts to refine peaks of residual electron density as disordered or partial-occupancy solvent dichloromethane chlorine or carbon atoms were unsuccessful. The data were corrected for disordered electron density through use of the SQUEEZE procedure [4a] as implemented in PLATON [4b,c]. A total solvent-accessible void volume of 1079.1 Å³ with a total electron count of 182 (consistent with four molecules of solvent dichloromethane, or one-half molecule per formula unit of the ruthenium complex molecule) was found in the unit cell.

3. Results and discussion

3.1. Synthesis of diastereomeric mixtures of **2**

The unsymmetrically-substituted secondary phosphine HPBu^tPh reacts with complex **1** in refluxing dichloromethane to give complete conversion to the mixed phosphine complex **2** in 3–4 h. After removal of the solvent under vacuum, $^{31}\text{P}\{^1\text{H}\}$ NMR spectroscopy of the resulting red oil consistently shows the presence of two diastereomers, **2a** and **2b**, in an approximate ratio of 60:40.^{2,3} Washing with hexanes gives **2** as an orange powder, still with a 60:40 mixture of **a** and **b**, as determined by $^{31}\text{P}\{^1\text{H}\}$ NMR recorded immediately after the sample is dissolved in NMR solvent (either *d*₁-chloroform or *d*₆-benzene). However, as shown in Fig. 1, over time in solution the diastereomer ratio shifts to give predominantly **2a**, indicating that (i) the diastereomers are in equilibrium and (ii) diastereomer **2a** is the more thermodynamically stable product.

Removal of the residual PPh₃ and HPBu^tPh from this orange powder requires either copious washing with hexanes or recrystallization from dichloromethane and hexanes. The latter technique gives dark red crystalline material that tends to be rich in **2b** relative to the “kinetic” 60:40 product distribution described above, with the highest relative amounts of **2b** being observed when the recrystallization takes place at low temperature in the freezer. Thus, while solution studies indicate the higher thermodynamic stability of **2a**, complex **2b** is the less soluble isomer. These differences present some interesting possibilities for obtaining one or both of the isomers in a pure form, which would allow us to study the kinetics of the approach to diastereomer equilibrium as a function of temperature. We continue to pursue this strategy for establishing the mechanism of epimerization, in particular to better understand the importance of associative versus dissociative substitution processes for this η^5 -indenyl system.⁴

3.2. NMR characterization of the diastereomers of **2**

The ^1H NMR spectra of **2a** and **2b** are sufficiently distinct to allow unequivocal assignment of peaks due to the P–H, indenyl, and Bu^t protons for each diastereomer in the mixtures we isolated (Table 1, Section 2.3), and the general attribution of aromatic peaks to either the PPh₃ or the secondary phosphine Ph for each diastereomer. Diagnostic P–H signals, centered between 5 and 6 ppm, exhibit the expected large, $^1J_{\text{PH}}$ coupling (362 Hz (**a**), 346 Hz (**b**)). The chirality at Ru renders diastereotopic the protons on either side of

² In a representative experiment, $^{31}\text{P}\{^1\text{H}\}$ NMR of an aliquot removed before reaction had gone to completion showed the same 60:40 ratio of **2a** and **2b**.

³ 202.5 MHz $^{31}\text{P}\{^1\text{H}\}$ data (δ) for **2** in *d*₁-chloroform: (**a**) 85.5 (d, $^2J_{\text{PP}}$ = 43 Hz, HPBu^tPh), 42.7 (d, PPh₃); (**b**) 70.2 (d, $^2J_{\text{PP}}$ = 43 Hz, HPBu^tPh); 51.4 (d, PPh₃).

⁴ Previous studies of phosphine substitution reactions at **1** point to predominantly dissociative pathways for this crowded, bis(PPh₃) complex, (see Ref. [3]) but nevertheless the importance of variable hapticity of the indenyl ligand in our systems remains an open question.

Table 2
125 MHz $^{13}\text{C}\{^1\text{H}\}$ NMR data at 300 K: δ in ppm (multiplicity, J_{PC} or $\omega_{1/2}$ in Hz).^a

	η^5 -Indenyl				PPh ₃ both isomers			HPBu ^t -Ph	
	C ₇ , C ₄	C ₆ , C ₅	C _{3a} , C _{7a}	$\Delta\delta$ (C _{3a} , C _{7a}) ^b	C ₂	C ₃ , C ₁		Ph	Bu ^t
2a	125.1 (s)	127.8 (s)	111.4 (br s, 10)	−20.6 (av)	81.2 (s)	65.4 (d, 13)	134.7–133.9 (br)	135.9 (d, 40)	37.2 (dd, 26, 4)
	124.0 (s)	126.8 (s)	108.9 (d, 6)			61.5 (s)	133.9–132.1 (br)	133.2 (d, 8)	
2b	125.1 (2 × s)	127.3 (s)	110.5 (br s, 6)	−20.8 (av)	84.6 (s)	64.4 (s)	129.5–128.7 (br om)	129.4 (dd, 18, 1)	30.2 (d, 4)
		127.25 (s)	109.3 (br s, 6)			64.1 (d, 8)	128.1–126.8 (overlapping, some br) br in baseline	127.9 (s)	
								133.0 (d, 6)	35.5 (d, 24)
								129.1 (d, 16)	29.9 (d, 4)
							127.7 (s)		

^a Samples in *d*₁-chloroform.^b $\Delta\delta$ (C_{3a}, C_{7a}) = δ (C_{3a}, C_{7a} (η -indenyl complex)) − δ (C_{3a}, C_{7a} (η -sodium indenyl)). δ (C_{3a}, C_{7a}) for sodium indenyl = 130.7 ppm [3].**Table 3**
Crystallographic data for $[(\eta^5\text{-indenyl})\text{Ru}\{\text{P}(\text{H}^t\text{Bu})\text{Ph}\}(\text{PPh}_3)] \cdot 0.5\text{CH}_2\text{Cl}_2$ (**2**).

Formula	C _{37.5} H ₃₈ Cl ₂ P ₂ Ru
Formula weight	722.59
Crystal color, habit	orange plate
Crystal dimensions (mm)	0.45 × 0.37 × 0.07
Crystal system, space group	orthorhombic, <i>Pbcn</i> (no. 60)
<i>a</i> (Å)	24.5725 (8)
<i>b</i> (Å)	19.1823 (7)
<i>c</i> (Å)	14.9657 (5)
<i>V</i> (Å ³)	7054.2 (4)
<i>Z</i>	8
<i>D</i> _{calcd} (g cm ^{−3})	1.361
μ (mm ^{−1})	0.711
Diffractometer	Bruker D8/APEX II CCD ^a
Radiation (λ [Å])	graphite-monochromated Mo K α (0.71073)
Temperature (°C)	−100
Data collection $2\theta_{\text{max}}$ (°)	55.02
Total data collected	60089 (−31 ≤ <i>h</i> ≤ 31, −24 ≤ <i>k</i> ≤ 24, −19 ≤ <i>l</i> ≤ 19)
Independent reflns (<i>R</i> _{int})	8127 (0.0284)
Observed reflections	7014
$[F_o^2 \geq 2\sigma(F_o^2)]$	
Structure solution method	Patterson/structure expansion (DIRDIF-2008 ^b)
Refinement method	Full-matrix least-squares on <i>F</i> ² (SHELXL-97 ^c)
Absorption correction method	Gaussian integration (face-indexed)
Range of transmission factors	0.9519–0.7416
Data/restraints/parameters	8127/0/374
Goodness-of-fit (GOF) (<i>S</i>) (all data) ^d	1.050
<i>R</i> ₁ [<i>F</i> _o ² ≥ 2σ(<i>F</i> _o ²)] ^e	0.0269
<i>wR</i> ₂ (all data) ^f	0.0669
Largest diff peak, hole (e Å ^{−3})	0.436, −0.662

^a Programs for diffractometer operation, unit cell indexing, data collection, data reduction and absorption correction were those supplied by Bruker.^b P.T. Beurskens, G. Beurskens, R. de Gelder, S. Garcia-Grandia, R. Israel, R.O. Gould, J.M.M. Smits, The DIRDIF-99 Program System, Crystallography Laboratory, University of Nijmegen, The Netherlands, 1999.^c G.M. Sheldrick, Acta Crystallogr., Sect. A 64 (2008) 112.^d $S = [\sum w(F_o^2 - F_c^2)^2 / (n - p)]^{1/2}$ (*n* = number of data; *p* = number of parameters varied; $w = [\sigma^2(F_o^2) + (0.0304P)^2 + 3.9411P]^{-1}$ where $P = [\text{Max}(F_o^2, 0) + 2F_c^2]/3$).^e $R_1 = \sum |F_o| - |F_c| / \sum |F_o|$.^f $wR_2 = [\sum w(F_o^2 - F_c^2)^2 / \sum w(F_o^4)]^{1/2}$.

the plane of symmetry bisecting the indenyl ligand: accordingly we see seven distinct signals for H1–H7 for both isomers. The sharpness of these signals indicates that rotation about the Ru–indenyl bond is either very fast or very slow on the NMR time-scale; we suspect the former, based on the four sharp indenyl proton signals we observe for the more symmetric, but comparably sterically crowded, parent complex **1**. Peaks due to the protons on the indenyl 5- and 6-rings in **2a** show more disperse chemical

shifts than those in **2b**, suggesting that the structure of **2a** places them in closer proximity to the phenyl groups on the PPh₃ and HPBu^tPh ligands, such that they experience greater ring-current shielding (or deshielding) effects. In particular, the signal due to one of the protons on the 5-ring in **2a** (H1 or H3 in the numbering scheme shown in Fig. 2) shows an extreme shift to high field (δ 2.70 ppm in *d*₁-chloroform, δ 2.81 ppm in *d*₆-benzene), consistent with its proximity to the center of a phenyl ring that lies perpendicular to the C–H1/3 bond axis. Similar to what we described previously for the complexes $[\text{Ru}(\eta^5\text{-indenyl})\text{Cl}(\text{PR}_2\text{H})(\text{PPh}_3)]$, where R = Cy or Ph [1], we observe broadening of many of the aromatic signals due to PPh₃ in the room temperature ¹H and (¹³C{¹H}) NMR spectra of mixtures of **2a** and **2b**. This arises from the combination of slowed rotation around the Ru–PPh₃ bond (due to steric congestion at ruthenium) and disparate chemical environments experienced by each of these three phenyl groups. The peak broadening is typically exacerbated for congested structures in which one PPh₃ phenyl group points directly toward the indenyl 6-ring, with particularly pronounced chemical shift dispersion being observed for H_{ortho}, C_{ipso}, and C_{ortho} in the ¹H and (¹³C{¹H}) spectra. The degree of broadening we observe for aromatic peaks due to **2a**, relative to those due to **2b**, suggests that the PPh₃ chemical shift dispersion is more pronounced for **2a** than for **2b**, which may indicate the PPh₃ is closer to the 6-ring of the indenyl ligand and/or to the P–H group on the HPBu^tPh ligand in **2a**.

3.3. Assignment of relative stereochemistries in diastereomers **2a** and **2b**

The recrystallization described in Section 3.1 gave us crystals of **2** suitable for analysis by X-ray diffraction. The resulting molecular structure is shown in Fig. 3, along with a simplified drawing to indicate the relative stereochemistries at Ru and the secondary phosphine. The P–H group of the secondary phosphine (H1P) lies approximately *anti* to the Ru–indenyl bond (Ru–C*) along the P1–Ru bond, which allows the Ph and Bu^t groups on the secondary phosphine to achieve maximum distance from the PPh₃ phenyl rings.⁵ These two groups lie on opposite sides of the plane containing H1P, P1, Ru, and C*, which bisects the indenyl ring and also contains H2. Relative to this plane, the phenyl group of the secondary phosphine is on the same “side” as the Cl ligand on Ru, while the Bu^t group is on the same side as the PPh₃ ligand.

Comparison of the solution ¹H NOESY NMR correlations for the diastereomer mixture (see Supporting Information) to the solid state structure shown in Fig. 3 allows us to propose an assignment

⁵ Similar to what we reported in Ref. [1] for the symmetrically substituted analogues of **2**, the crystallographic and IR data obtained for **2** provide no evidence for hydrogen bonding between the secondary phosphine P–H and the Ru–Cl.

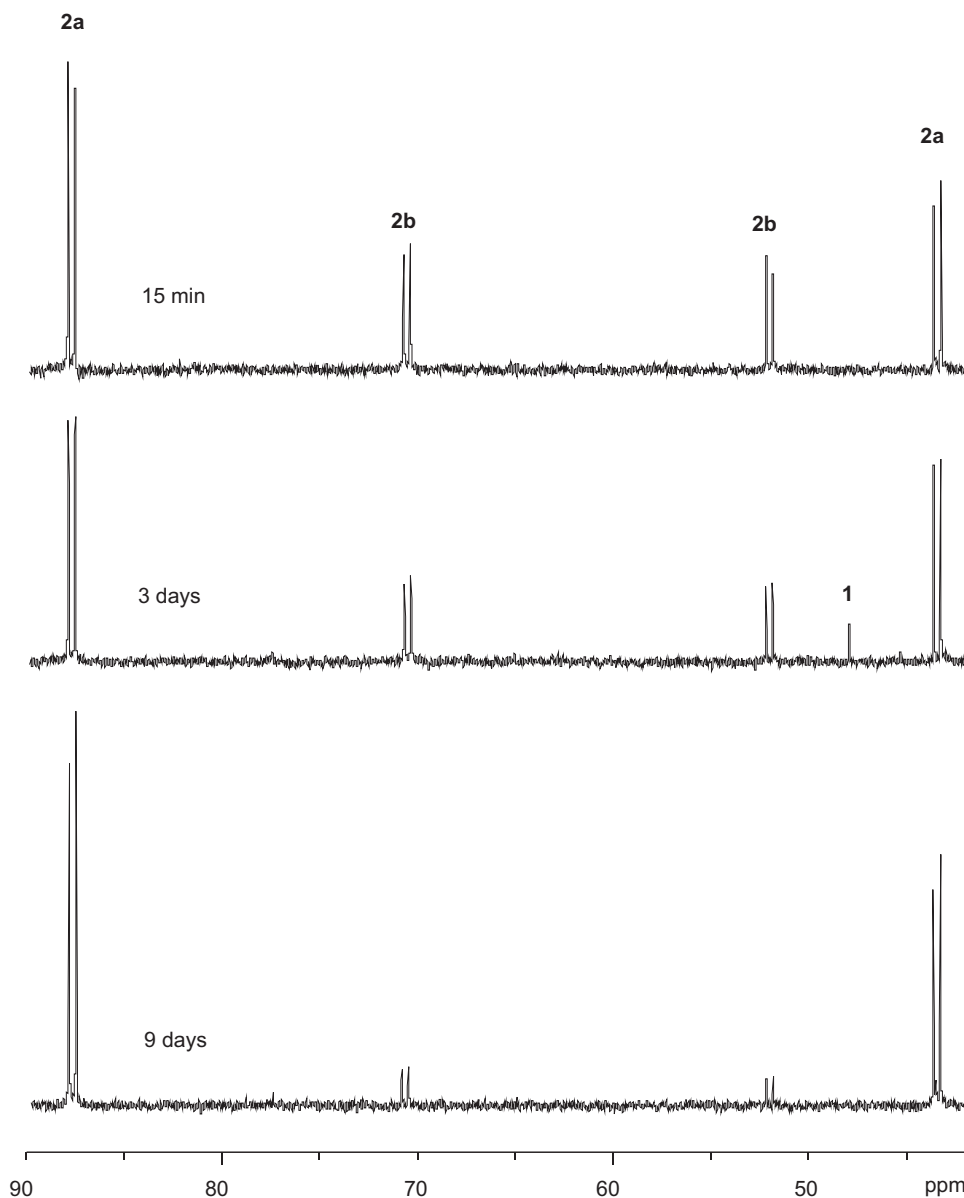


Fig. 1. 121.49 MHz $^{31}\text{P}\{^1\text{H}\}$ NMR spectra of a mixture of **2a** and **2b** in d_6 -benzene in a J. Young sealable NMR tube at room temperature (a small amount of residual PPh_3 (-5 ppm) apparently reacts with **2** to give a small amount of **1** (47 ppm), which is in equilibrium with **2**. Ultimately this excess PPh_3 is completely converted to $\text{O}=\text{PPh}_3$ (26 ppm) by reaction with trace oxygen in the sample.).

of the distinct spectra for **2a** and **2b** to structures of defined relative stereochemistry. For both isomers, signals due to the P–H groups show correlation with PPh_3 signals but not with any signals due to indenyl protons. (The P–H group for **2b** also shows a correlation with signals due to the P–H group of the secondary phosphine.) This supports a solution conformation for both isomers that conserves, at least approximately, the *anti* relationship of the P–H and Ru–indenyl bonds, as observed in the solid state structure. Thus the secondary phosphine Ph and Bu^t substituents must sit “up” toward the η^5 -indenyl ligand in both isomers, with one pointing to the same side as the Cl ligand and the other pointing toward the side of the PPh_3 ligand. NOESY correlations for the indenyl H1 and H3 signals (which are well separated in the spectra of both isomers) are therefore quite diagnostic of the stereochemistry at the secondary phosphine, since one of H1 and H3 must point to the PPh_3 side of the complex and the other must point toward the Cl side of the complex. As illustrated in Fig. 4, for **2a** the downfield H1/3 signal shows a correlation only with the Bu^t signal, while the upfield H1/3 signal shows correlations with both secondary

phosphine Ph and PPh_3 signals (presumably H_{ortho}). The H2 signal for **2a** shows correlations with the Bu^t and PPh_3 signals and a weak correlation with the secondary phosphine Ph signal. For **2b**, the downfield H1/3 signal correlates with signals due to PPh_3 and correlates weakly to the Bu^t signal, while the upfield H1/3 signal correlates with signals due to the secondary phosphine Ph and correlates weakly to the Bu^t signal. The H2 signal for **2b** shows correlations with signals due to all three of the Bu^t , secondary phosphine Ph, and PPh_3 groups. Based on these correlations, which establish the relative positions of the secondary phosphine Ph and the PPh_3 ligand on either “side” of the indenyl ring for both isomers, we propose that the relative stereochemistry we observe in the solid state structure corresponds to the structure of **2b**,⁶ in which the secondary phosphine Ph lies toward the Cl side of the mol-

⁶ The solution structure of **2b** has a slightly different conformation from the solid state structure: in the NOESY spectrum we see weak correlations of both H1 and H3 with the Bu^t protons, which are consistent with a minimum H1– Bu^t distance of 2.848 Å (H1–H19B) but not with a minimum H3– Bu^t distance of 4.431 Å (H3–H19A).

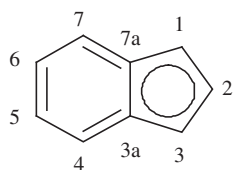


Fig. 2. Numbering system used for the indenyl ligand.

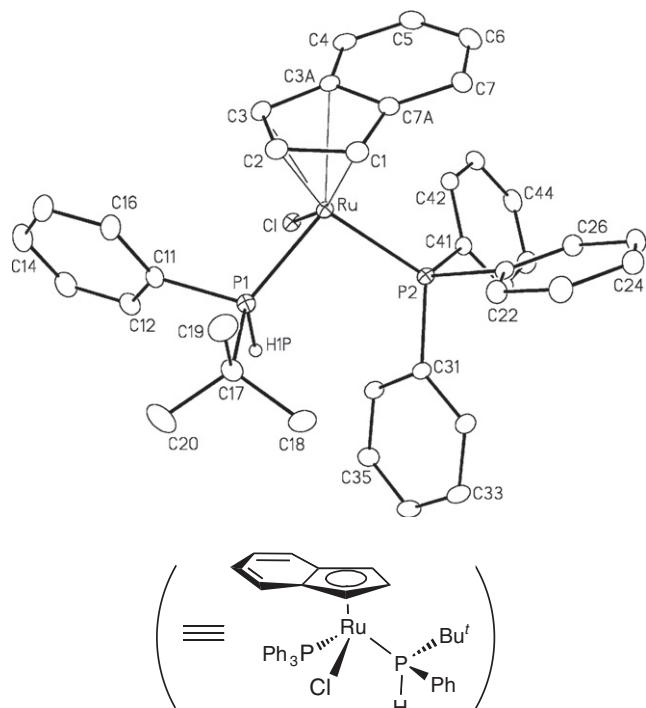


Fig. 3. Molecular structure of **2**, assigned as **2b**. Non-hydrogen atoms are represented by Gaussian ellipsoids at the 20% probability level. The hydrogen atom attached to P1 is shown with an arbitrarily small thermal parameter; all other hydrogens are not shown. Selected interatomic distances (Å) and bond angles (deg) (C^* denotes the centroid of the plane defined by C(7A)–C(1)–C(2)–C(3)–C(3A)): Ru–P(1) = 2.2618(5), Ru–P(2) = 2.3242(4), Ru–Cl = 2.4366(4), Ru–C* = 1.895, P(1)–H(1P) = 1.292(18); P(1)–Ru–P(2) = 97.941(16), P(1)–Ru–Cl = 81.610(15), P(2)–Ru–Cl = 87.346(14), P(1)–Ru–C* = 125.2, P(2)–Ru–C* = 126.1, Cl–Ru–C* = 125.6. Indenyl slip distortion: $\Delta = d[\text{Ru}-\text{C}(7\text{A}),\text{C}(3\text{A})] - d[\text{Ru}-\text{C}(1),\text{C}(3)] = 0.141 \text{ \AA}$.

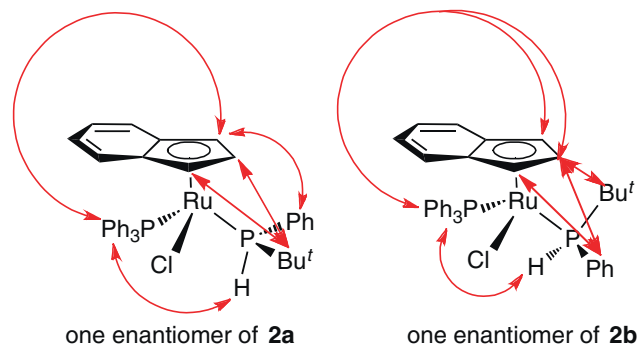


Fig. 4. Structures of **2a** and **2b** indicating the relative stereochemistry at ruthenium and the secondary phosphine for each diastereomer. The double-headed arrows indicate groups for which ^1H NOE correlations are observed.

the molecule is particularly rich in aromatic groups relative to the other side.

4. Conclusion

The utility of chiral-at-metal complexes in studying the reaction mechanisms of transition metal complexes, and their potential for introducing stereocontrol in catalytic systems, has been well-established by Brunner and others, and chiral ruthenium half-sandwich complexes have played a large role in the development of this field [5]. Complex **2** represents an important new example of a relatively configurationally stable system undergoing epimerization at rates that will allow mechanistic study by NMR. It is also an unusual example of diastereoisomerism involving the metal coordination of (racemic mixtures) of P-chiral secondary phosphines [6], of relevance to the increasing interest in stereoselective synthesis of P-chiral phosphine ligands via catalytic P–C bond-forming reactions [7]. In this context, we are currently studying the base-promoted dehydrohalogenation of complex **2**; preliminary experiments confirm the formation of stereoisomers of the corresponding terminal phosphido complex $[\text{Ru}(\eta^5\text{-indenyl})(=\text{P}^i\text{Bu}^t\text{Ph})(\text{PPh}_3)]^2$ (**3**, **3'** in a 1:7 ratio), which exhibit the diagnostic deep blue color of these 5-coordinate complexes [2c] and are relatively stable at room temperature in solution ($\sim\text{h}$).⁸ We will report more on these results in due course.

Acknowledgment

We thank the Natural Sciences and Engineering Research Council (NSERC) of Canada for funding.

Appendix A. Supplementary material

Supplementary data associated with this article can be found, in the online version, at doi:10.1016/j.ica.2010.12.058.

References

- [1] E.J. Derrah, J.C. Marlinga, D. Mitra, D.M. Friesen, S.A. Hall, R. McDonald, L. Rosenberg, *Organometallics* 24 (2005) 5817.
- [2] (a) E.J. Derrah, K.E. Giesbrecht, R. McDonald, L. Rosenberg, *Organometallics* 27 (2008) 5025; (b) E.J. Derrah, R. McDonald, L. Rosenberg, *Chem. Commun.* 46 (2010) 4592; (c) E.J. Derrah, D.A. Pantazis, R. McDonald, L. Rosenberg, *Organometallics* 26 (2007) 1473; (d) E.J. Derrah, D.A. Pantazis, R. McDonald, L. Rosenberg, *Angew. Chem., Int. Ed.* 49 (2010) 3367.
- [3] M.P. Gamasa, J. Gimeno, C. GonzalezBernardo, B.M. MartinVaca, D. Monti, M. Bassetti, *Organometallics* 15 (1996) 302.
- [4] (a) P. Vandersluijs, A.L. Spek, *Acta Crystallogr., Sect. A* 46 (1990) 194; (b) A.L. Spek, *J. Appl. Crystallogr.* 36 (2003) 7; (c) PLATON, A Multipurpose Crystallographic Tool, Utrecht University, Utrecht, The Netherlands.
- [5] (a) H. Brunner, *Adv. Organomet. Chem.* 18 (1980) 151; (b) G. Consiglio, F. Morandini, *Chem. Rev.* 87 (1987) 761; (c) H. Brunner, *Angew. Chem., Int. Ed.* 38 (1999) 1195; (d) H. Brunner, *Eur. J. Inorg. Chem.* (2001) 905; (e) H. Brunner, M. Weber, M. Zabel, *Coord. Chem. Rev.* 242 (2003) 3; (f) H. Brunner, T. Tsuno, *Acc. Chem. Res.* 42 (2009) 1501.
- [6] (a) E. Hey, A.C. Willis, S.B. Wild, *Z. Naturforsch. B* 44 (1989) 1041; (b) A. Bader, T. Nullmeyers, M. Pabel, G. Salem, A.C. Willis, S.B. Wild, *Inorg. Chem.* 34 (1995) 384; (c) D.K. Wicht, I. Kovacic, D.S. Glueck, L.M. Liable-Sands, C.D. Incarvito, A.L. Rheingold, *Organometallics* 18 (1999) 5141; (d) C. Scriban, D.S. Glueck, A.G. DiPasquale, A.L. Rheingold, *Organometallics* 25 (2006) 5435;

⁷ 202.5 MHz $^{31}\text{P}\{^1\text{H}\}$ data (δ) for **3** and **3'** in d_6 -benzene: (**3**) 257.7 (d, $^2J_{\text{PP}} = 60 \text{ Hz}$, $\text{P}^i\text{Bu}^t\text{Ph}$), 61.5 (d, PPh_3); (**3'**) 253.3 (d, $^2J_{\text{PP}} = 60 \text{ Hz}$, $\text{P}^i\text{Bu}^t\text{Ph}$); 60.7 (d, PPh_3).

⁸ Decomposition in solution leads principally to the products of orthometallation [2c], **4** and **4'**, in a 1:1.3 ratio. 121.5 MHz $^{31}\text{P}\{^1\text{H}\}$ data (δ) for **4** and **4'** in d_6 -benzene: (**4**) 83.4 (d, $^2J_{\text{PP}} = 26 \text{ Hz}$, $\text{HP}^i\text{Bu}^t\text{Ph}$), -18.6 (d, $\text{PPh}_2\text{C}_6\text{H}_4$); (**4'**) 76.6 (d, $^2J_{\text{PP}} = 29 \text{ Hz}$, $\text{HP}^i\text{Bu}^t\text{Ph}$); -21.4 (d, $\text{PPh}_2\text{C}_6\text{H}_4$).

ecule, while for **2a** the secondary phosphine Ph lies toward the PPh_3 side of the molecule. This latter relative stereochemistry is consistent with the extreme ^1H chemical shift dispersion we observe for both the indenyl protons and the PPh_3 protons, since one side of

(e) N.F. Blank, J.R. Moncarz, T.J. Brunker, C. Scriban, B.J. Anderson, O. Amir, D.S. Glueck, L.N. Zakharov, J.A. Golen, C.D. Incarvito, A.L. Rheingold, *J. Am. Chem. Soc.* 129 (2007) 6847;

(f) V.S. Chan, M. Chiu, R.G. Bergman, F.D. Toste, *J. Am. Chem. Soc.* 131 (2009) 6021.

[7] D.S. Glueck, *Top. Organomet. Chem.* 31 (2010) 65.